Journal of Chromatography B, 889–890 (2012) 95–102

Contents lists available at SciVerse ScienceDirect

Journal of Chromatography B

journal homepage: www.elsevier.com/locate/chromb

Molecular imprinting based composite cryogel membranes for purification of anti-hepatitis B surface antibody by fast protein liquid chromatography

Sevgi Asliyuce[a], Lokman Uzun[a,*], Abbas Yousefi Rad[b], Serhat Unal[c], Ridvan Say[d], Adil Denizli[a]

[a] Hacettepe University, Department of Chemistry, Biochemistry Division, Ankara, Turkey
[b] TOBB ETU Hospital, Ankara, Turkey
[c] Hacettepe University, Faculty of Medicine, Ankara, Turkey
[d] Anadolu University, Department of Chemistry, Eskişehir, Turkey

ARTICLE INFO

Article history:
Received 7 October 2011
Accepted 3 February 2012
Available online 9 February 2012

Key words:
Molecular imprinted polymers
Anti-hepatitis B surface antibody
Composite cryogel membrane
Fast protein liquid chromatography
Affinity purification

ABSTRACT

In the present study, we have focused our attention to prepare molecular imprinted composite cryogel membranes for purification of hepatitis B surface antibody (anti-HBs) by fast protein liquid chromatography. Before the preparation of the molecular imprinted composite cryogel membranes (MI-CMs) by free radical polymerization at sub-zero temperature, we have synthesized and characterized the anti-HBs imprinted particles. Then, the cryogel membranes (CMs) were characterized by swelling test, scanning electron microscopy and Fourier transform infrared spectroscopy. Prior to chromatographic purification studies, the effective parameters on the anti-HBs adsorption process were evaluated by investigating the dependency of the adsorption capacity on flow-rate, anti-HBs concentration, contact time and ionic strength. The maximum anti-HBs adsorption capacity was calculated as 701.4 mIU/g CM. The selectivity of the MI-CMs was shown by competitive adsorption of anti-HBs, total anti-hepatitis A antibody (anti-HAV) and total immunoglobulin E (IgE) adsorption studies. The MI-CMs have relative selectivity coefficients as 5.45 for anti-HBs/total anti-HAV and 9.05 for anti-HBs/total IgE, respectively. The phosphate buffer solution (pH 7.4) containing 1.0 M NaCl was used for elution, almost completely, of adsorbed anti-HBs molecules. The MI-CMs could be used many times without any significant decrease in the adsorption capacity. The chromatographic purification performances of the MI-CMs were also investigated. The chromatographic parameters such as capacity and separation factors, the theoretical plate number and resolution of the MI-CMs were calculated as 5.48, 6.02, 1153.9, and 1.72 for anti-HBs molecules, respectively. As a conclusion, we can say that the MI-CMs could be used for specific purification of anti-HBs from anti-HBs positive human plasma.

1. Introduction

The prevalence of hepatitis B virus (HBV) infection is getting wider as the day goes on although an extensive vaccination has been applied [1]. Due to 75% of the world's population living in areas having high infection level and more than 350 million people are chronic carriers, the governments have to apply and set a huge budget for the preventive vaccination [2,3]. Not only diseases directly related to acute HBV infection but also associated with diseases such as liver cirrhosis and hepatocellular carcinoma depending on chronic HBV development are important global health problem concerns [4]. Especially in case of infants born to hepatitis B positive mothers, the fatal chronic disease development is potentially occurred [5]. For prevention of these infants, they are immunized passively by giving high titer neutralizing antibodies, anti-hepatitis B surface antibodies (anti-HBs), against to antigenic determinants on HB viruses immediately after birth. In the following 2–5 months, HBs vaccines should be repeated several times [6]. In addition to the infants, a considerable numbers of people at high risk of HBV infection are required to be immunized passively against to HBV infection because they are not protected during the first month after vaccination. An immediate protection should be introduced to these people such as patients and personals in dialysis unit, close contacts of chronic HBV carriers, tourist gone to where high HBV prevalence etc. after accidental inoculation with infectious materials, needle stick or other means [7]. The antibodies transferred passively prepared from the sera of anti-HBs positive donors according to regulations assured by strict product standard, prevents the infection during the period of development of an active immune response [8].

Anti-HBs containing sera are prepared not only from anti-HBs positive donors but also from immunized animal plasma and transgenic plants [4]. The purification system was mainly based on protein A affinity chromatography used widely for antibody

* Corresponding author. Tel.: +90 312 297 7963; fax: +90 312 299 2163.
E-mail address: lokman@hacettepe.edu.tr (L. Uzun).

1570-0232/$ – see front matter © 2012 Elsevier B.V. All rights reserved.
doi:10.1016/j.jchromb.2012.02.001

purification protocols [9–13]. Hernandez et al. purified anti-HBs from ascites fluid of immunized mice by Sepharose CL-4B-protein A adsorbent [9]. Mouta Junior et al. purified anti-HBs polyclonal and monoclonal antibodies by Affi-Prep protein A MAPS II [10]. Protein A-Sepharose columns were used for antibody purification from transgenic tobacco clon HCLC-23 lead extracts [11,12]. Poros protein A plastic column was also used for anti-HBs purification from transgenic tobacco cells [13]. Protein A adsorbents show high selectivity and can therefore be employed as a one-step procedure for the purification of antibodies in pilot scale. However, in spite of its high selectivity, protein A adsorbents has some difficulties which are worth considering: (i) a considerable amount of protein A may release from the matrix and resulted contamination cannot unfortunately be tolerated in clinical applications and (ii) the cost of protein A adsorbents remains high. In addition, it is difficult to immobilize protein A in suitable orientation [14,15]. Molecular imprinted polymer (MIP) based adsorbents are promising alternatives to conventional protein A based adsorbents because of their simplicity, universality, stability and cheapness [16]. MIPs should also display not only reduced production costs at large scale purification, but also increased resistance to chemical and biological actions [17].

During last decades, the numbers of publication related with molecular imprinting technology are growing rapidly and the molecular imprinting based adsorbents are studied intensively [18]. In this technology, the molecule interested in to separate, purify or detect are imprinted into highly cross-linked polymeric network [19]. Because of extensive efforts on preparation of new imprinted polymers, discussions on the advantages and drawbacks of the applied approaches, especially for imprinting of biological macromolecules such as proteins, are the main issues for researchers [20,21]. Hereby, some problems such as denaturation and conformational change tendency of proteins, probable non-specific interactions occurred because of large number of binding sites on the protein surface should be overcome during protein imprinting process [22,23]. Protein imprinting while cryogelation is one of the alternative polymerization techniques [24]. The cryogelation is promising polymerization approach to prepare hydrogels classified as continuous separation media having large inter-connected flow-channels at subzero temperature [25]. During the cryogelation, the protein conformation dynamics and the denaturation problems were limited because the polymerization was taken out at lowered temperature [24]. The obtained hydrogels called as cryogels allow the users to study at high flow-rates without significant pressure drop and diffusion resistance because of their supermacroporous structure. The short process time and possibility of whole blood application without any pre-treatment are other advantages of these adsorption media [26]. Despite of the fact that cryogels have several advantages; the main problem to deal is low specific surface area that causes lower adsorption capacities. Embedding of small particles into cryogel structure or direct cryogelation of particles are encouraging alternatives to deal the problem [26–29].

In the present study, we have focused our efforts on preparation of molecular imprinting based cryogel membranes and using them for fast protein liquid chromatographic (FPLC) purification of anti-HBs from human plasma. In the first part of the study, the preparation and characterization of anti-HBs imprinted polymers were reported in our previous study [4]. In second part, anti-HBs imprinted particles were embedded into cryogel membranes to prepare continuous separation media for FPLC application. Swelling test, scanning electron microscopy and Fourier transform infrared spectroscopy were applied to characterize the anti-HBs imprinted composite cryogel membranes (MI-CM). In order to evaluate the purification performance of MI-CMs, the effective factors such as flow-rate, anti-HBs concentration, ionic strength, etc. were investigated. In the last step, we have performed liquid chromatographic purification of anti-HBs molecules from human plasma by attaching the MI-CMs to FPLC system.

Table 1
Some physical and chemical properties of the embedded particles.

	Anti-HBs imprinted particles	Non-imprinted particles
Surface area (m^2/g)	20.2	9.3
Average pore diameter (Å)	22.8	21.8
MAT content (μmol/g)	6.1	5.8
Particle size (μm)	20–63	20–63

2. Experimental

2.1. Materials

Anti-hepatitis B surface antibody (anti-HBs) was supplied from Chemicon (Hampshire, England), L-tyrosine methyl ester, methacryloyl chloride, potassium persulfate (KPS), 3-(N-morpholino)propane sulphonic acid (MOPS) were obtained from Sigma Chemical Co. (St. Louis, USA). Hydroxyethyl methacrylate (HEMA) and ethylene glycol dimethacrylate (EGDMA), N,N,N′,N′-tetramethylene diamine (TEMED) and ammonium persulfate (APS) were purchased from Fluka A.G. (Buchs, Switzerland). HEMA and EGDMA were distilled under reduced pressure in the presence of hydroquinone inhibitor and stored at 4 °C until use.

2.2. Preparation of anti-HBs imprinted polymer

Anti-HBs imprinted polymers were prepared and characterized as reported in our previous study [4]. The applied procedure can be summarized as: anti-HBs (i.e. template) and functional monomer (MAT), the polymerizable derivative of the L-tyrosine methyl ester, were mixed with 1.0 mL of MOPS buffer (pH 6.0) and the mixture was stirred at room temperature for 2 h. Then, anti-HBs imprinted polymer was prepared in the presence of cross linker (EGDMA, 1 mL), functional monomer (HEMA, 3 mL), porogen (toluene, 2 mL) and template. The mixture was placed in a test tube and KPS (0.05 g) was added into this solution. The mixture was then bubbled with nitrogen gas for 5 min. The plastic syringe was sealed and vortexed for 2 min. The bulk polymerization procedure was continued at 40 °C for 1 h. The molecularly imprinted polymer obtained was dried, grounded into particle form and sieved (particle size 20–63 μm). Non-imprinted polymer was prepared according to the same recipe without anti-HBs in the polymerization medium. Some physical and chemical properties of the embedded particles were summarized in Table 1 [4].

2.3. Preparation of particle embedded cryogel membranes

Anti-HBs imprinted composite cryogel membranes were prepared as follows: the main monomer (10 mL HEMA) were dissolved in deionized water and the mixture was degassed under vacuum (100 mmHg) for about 5 min to eliminate soluble oxygen. Total concentration of monomers was 12% (w/v). The composite cryogel membranes (CM) were produced by free radical polymerization initiated by redox-couple TEMED and APS. After adding APS [100 mg, 1% (w/v) of the total monomers], the solution was cooled in an ice bath for 2–3 min. TEMED [120 μL, 1% (w/v)] was added and the reaction mixture was stirred for 1 min. In this step, anti-HBs imprinted particles were introduced in the polymerization mixture (50 mg). Then, the reaction mixture was poured between two glass plates (25 cm × 25 cm). The polymerization solution in the glass plates was frozen at −16 °C for 24 h and then thawed at room

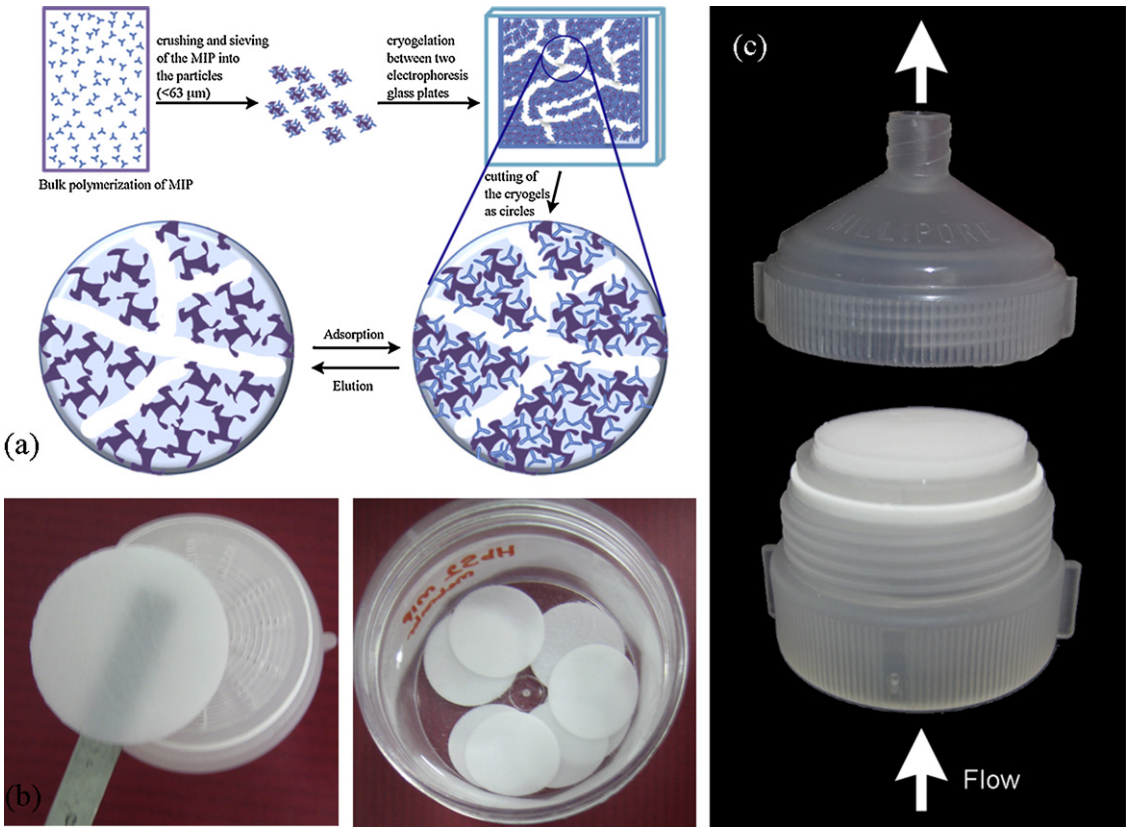

Fig. 1. (a) Schematic representation of applied polymerization steps; (b) optical pictures of CMs; and (c) the continuous operation setup.

temperature. The CMs obtained were cut into circular pieces (25 mm in diameter) with a perforator. The non-imprinted composite cryogel membranes (CMs) were prepared in the same way differently by using non-imprinted particles instead of imprinted ones. The CMs prepared were extensively washed with ethanol and water to remove any unreacted monomer or initiator and then stored in sodium azide 0.02% at 4 °C.

2.4. Characterization of particle embedded cryogel membranes

The swelling degree of the CMs (SD) was determined as follows: The CMs were dried until reaching constant weight at room temperature. Then, they were transferred to pre-weighed vial and weighed (W_0). After interacting them with water in a beaker (50 mL), we allowed them to reach to swollen state (W_1). The swelling degree was calculated as:

$$\mathrm{SD} = \frac{(W_1 - W_0)}{W_0} \quad (1)$$

The cross section and the surface morphology of the CMs were investigated with scanning electron microscope (SEM). The cryogels were initially dried in air at 25 °C for seven days before being analyzed. A fragment of the dried CMs was mounted on a SEM sample holder and was sputtered for gold film coating for 2 min. The sample was then mounted in a SEM (FEI Quanta 200 FEG, Oregon, USA). The surface of the CMs was scanned at the desired magnification to study the morphology of the CMs. FTIR spectroscopy was also used to characterize the chemical structure of MI-CMs in the solid state (Perkin Elmer, Spectrum one, USA). CM samples were dried in air at 25 °C for seven days before analysis, and then, pressed into pellet form by mixing with infrared grade potassium bromide (KBr, 100 mg) and the spectrum were recorded in a wavenumber range of 4000–450 cm^{-1}.

2.5. Anti-HBs adsorption–desorption experiments

Adsorption studies were performed with anti-HBs and anti-hepatitis A antibody (anti-HAV) positive human plasma. Anti-HBs and anti-HAV positive bloods were taken into the tubes containing EDTA. In order to get rid of blood cells, the samples were centrifuged at 4000 rpm at room temperature for 30 min. As the next step, the plasma sample was passed from 3 μm filter and stored in a deep freeze at −20 °C. Before use, the plasma sample was thawed at 37 °C for 1 h. The plasma sample was diluted with isotonic solution (0.9% NaCl solution) before used for experiments. Dilution ratio was changed from 1/5 to 1/100. Initial anti-HBs and total anti-HAV values were 895 mIU/mL and 490 mIU/mL, respectively. The diluted plasma samples (10.0 mL) were interacted with MI-CMs through continuous adsorption setup by means of placing the MI-CMs into a membrane holder (i.d. 25 mm, Sartorius, Aubagne, France) (Fig. 1). The solution feeding was performed by using a peristaltic pump (Watson-Marlow, Wilmington, MA, USA). The flow rate of feeding solution was changed between 0.5 mL/min and 2.0 mL/min. The anti-HBs concentration was varied in the range of 9.0–180.0 mIU/mL by diluting plasma samples in different ratios. The anti-HBs adsorption onto the CMs has been monitored for 120 min in order to determine optimum contact time between the CMs and anti-HBs molecules. The salt concentration of feeding solution was changed between 0.01 M and 0.50 M to investigate the effect of ionic strength on adsorption process. The amount of anti-HBs was determined by microparticle enzyme immunokit technology based AxSYM immunokit system (Abbott Laboratories, Abbott Park, IL, USA). All the analysis was performed according to the experimental procedures owned from producer company. The plasma samples having the minimum or higher positive values were accepted as reactive and the measurements were performed three times. The adsorbed amount of anti-HBs

per unit gram of CM was calculated according to the mass balance.

2.6. Selectivity experiments

In order to determine the selectivity of the MI-CMs, anti-HBs, total anti-HAV and total immunoglobulin E (IgE) adsorption from anti-HBs and anti-HAV positive plasma was investigated under competitive conditions. Plasma sample was prepared as mentioned before. The initial anti-HBs, total anti-HAV and total IgE values were 895, 490 and 5000 mIU/mL, respectively. Diluted plasma samples (5.0 mL) have been circulated through MI- and NI-CMs for 2 h. The total anti-HAV concentration was determined as anti-HBs according to producer's regulations. The total amount of IgE was determined by enzyme linked immunosorbent assay (ELISA) method. Detection kit is worked in accordance with fluorescent sandwich method enzyme immunokit (ELIFA) principle. Detections were performed using Mini Vidas system (Biomerieux, Marcy L'Etoile, France). Detection is based on IgE strip and solid phase cell (Solid Phase Receptacle). Strips contain many lanes for sample conjugates, for buffer, for reaction and finally for reading cell at last. Solid Phase Receptacles (SPRs) were coated with monoclonal anti-IgE antibody. Different strip and SPR were used for each sample. Sample (100 μL) was pipetted into the sample lane. All the detection procedures were completed automatically in 30 min by means of the instrument. Relative fluorescence values (REV) and the results were automatically calculated. The instrument used calibration curves and the concentration values were obtained as mIU/mL according to the international standards.

Distribution and selectivity coefficients for total anti-HAV and total IgE with respect to anti-HBs were calculated according to the following equation:

$$K_d = \left[\frac{(C_i - C_f)}{C_f}\right] \times \frac{V}{m} \quad (2)$$

In this equation, K_d represents the distribution coefficient (mL/mIU); C_i and C_f represents the initial and final concentration of anti-HBs (mIU/mL), V is the plasma volume (mL) and m is the mass of CM (g).

In the presence of interfering molecules, the selectivity coefficient for a template molecule (k) can be obtained from the binding data according to Eq. (3):

$$k = \frac{K_{d_{\text{template molecule}}}}{K_{d_{\text{interfering molecule}}}} \quad (3)$$

k values allow to interpret on imprinting selectivity. The relative selectivity coefficient (k') can be defined by Eq. (4):

$$k' = \frac{k_{\text{imprinted}}}{k_{\text{control}}} \quad (4)$$

2.7. Desorption and repeated use

The adsorbed anti-HBs molecules were desorbed using 100 mM phosphate buffer containing 1.0 M NaCl (pH 7.4). In a typical desorption experiment, 50 mL of the elution agent was pumped through the MI-CMs at a flow rate of 1.0 mL/min for 1 h. The final concentration of anti-HBs in the eluant was determined as mentioned above.

In order to show the reusability of MI-CMs, anti-HBs adsorption–elution procedure was repeated 10 times by using the same CM. In order to regenerate the MI-CM, it was sterilized with 50 mM NaOH solution after each adsorption–desorption cycle.

2.8. Chromatographic purification of anti-HBs

In this part of the study, we have connected the MI-CM to fast protein liquid chromatography system (FPLC). FPLC separation was performed using an AKTA-FPLC (Amersham Bioscience, Uppsala, Sweden) system equipped with a UV detection system. The system includes M-925 mixer, P-920 pump, UPC-900 monitor, INV-907 injection valve and Frac920 fraction collector. The MI-CM was equilibrated with 100 mM phosphate buffer (pH 7.4). A linear gradient of the buffer containing sodium chloride in range of 0–1 M was maintained at a flow rate of 1.0 mL/min. All buffers solutions were filtered before use. Anti-HBs positive plasma samples (2.0 mL) diluted in different ratio was applied to the system. Absorbance was monitored at 280 nm. The separation was performed at room temperature. KBr was used as the void marker. The peaks for both areas, bound and unbound regions, were collected by using Frac920 collector of the FPLC system and then the anti-HBs concentrations of the peaks were determined as mentioned before.

In order to evaluate the chromatographic performance of the MI-CMs, capacity (CF) and separation factors (α) were calculated as;

$$\text{CF} = \frac{(t_R - t_o)}{t_o} \quad (5)$$

$$\alpha = \frac{k'_2}{k'_1} \quad (6)$$

where, t_R is the retention time of the separated molecules, t_o is the retention time of the void marker (KBr), the CF_2 is capacity factor for anti-HBs and the CF_1 is capacity factor for competitors. The resolution (R_s) and theoretical plate number (N) were calculated using the following equations:

$$N = 5.54\left(\frac{t_R}{w_{0.5}}\right)^2 \quad (7)$$

$$\text{Rs} = \left(\frac{2(t_{R,2} - t_{R,1})}{(w_2 + w_1)}\right) \quad (8)$$

where $w_{0.5}$ is the peak height at the corresponding peak height fraction, $t_{R,1}$ and $t_{R,2}$ are the retention times of two adjacent peaks, w_1 and w_2 are the widths of the two adjacent peaks at the baseline.

3. Results and discussion

3.1. Characterization studies

Anti-HBs imprinted cryogel membranes were produced by cryogelation between two glass plates. As mentioned before, we have embedded the anti-HBs imprinted particles into the cryogel structure. By this way, we aimed to improve the chromatographic performance and to increase the specific surface area of the CMs. In addition, the particle embedded into the cryogel structure not only causes the increase the specific surface area but also retains the favourable properties of the cryogel structure such as large inter-connected flow channels, low back pressure, low diffusion resistance even at high flow-rates. The obtained CMs are opaque, sponge-like and have enough stability for column applications (Fig. 1). The equilibrium swelling degree of the MI-CMs was determined as 5.44 g H_2O/g CM while that of NI-CMs was 5.23 g H_2O/g CM, respectively. The higher swelling degree observed for MI-CMs can be explained by different ways. First, the imprinted particles have larger specific surface area than non-imprinted particles have [4]. Therefore, the surface area increase in embedded particles causes the surface area increase for the CMs. Second, the presence of molecular cavities in the imprinted particles can cause larger hydrodynamic volume to MI-CMs. Hereby, water molecules can

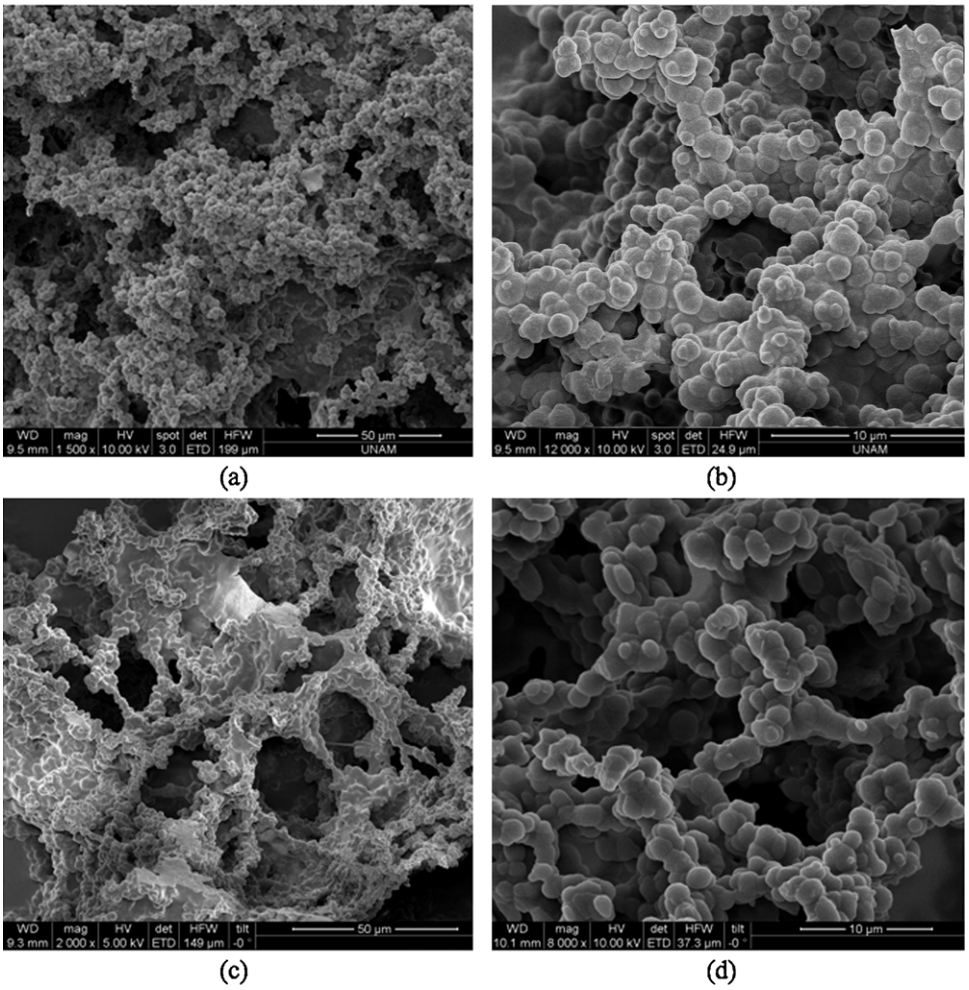

Fig. 2. Scanning electron photographs of (a and b) MI-CMs and (c and d) NI-CMs.

easily penetrate into polymeric chain of the cryogel membrane in the case of MI-CMs.

The scanning electron photographs of the internal structures of the MI-CMs and NI-CMs are shown in Fig. 2. The CMs prepared at −16 °C had numerous inter-connected large pores in the range of 20–200 μm. These pores could act as a channel for the mobile phase to flow easily through. Pore size of the CMs is much larger than the effective molecular radius (≈5.5 nm) of whole antibody molecules [30]; so then, it can pass easily through the pores. As a result of the convective flow achieved of the mobile phase through inter-connected pores, it is possible to study at higher flow-rate due to negligible mass transfer resistance. Fig. 2 also shows that the particles both imprinted and non-imprinted were successfully embedded into cryogel structure meanwhile interconnected supermacropores had been retained as expected. In addition, the embedded particles were polymerized very close to cryogel surface this case provides a rapid adsorption dynamics with higher adsorption capacities [26].

FTIR spectroscopy has been applied to characterize the chemical structure of MI-CMs and NI-CMs (Supplementary Material, SM-Fig. 1). MI-CMs have vibrational bands stemmed from the main monomer 2-hydroxyethyl methacrylate, as —OH stretching at 3430 cm^{-1}, aliphatic —CH stretching at 2952 cm^{-1}, and —C=O stretching at 1726 cm^{-1}, respectively [31]. In addition, MI-CMs also have vibrational bands originated from embedded particles. These bands can be listed as carboxyl —C—O— stretching and out of phase —NH rocking bands around 1454 cm^{-1}; —OH bending (phenol ring of tyrosine group), —C—H twist (aromatic ring) and —NH rocking at 1248 cm^{-1} and 1076 cm^{-1}; —C—H bending (out-of-plane) at 1159 cm^{-1} and 1024 cm^{-1}; and chain asymmetric stretching at 900 cm^{-1}, respectively [32]. Similarly, NI-CMs have almost same FTIR bands with MI-CMs because of chemical structural similarities of polymeric backbones and same functional monomer used for preparation of the particles embedded into cryogel structure.

3.2. Anti-HBs adsorption from human plasma

3.2.1. Effect of flow-rate

The adsorption dependency on flow-rate of the MI-CMs is given in Fig. 3. The results show that the amount of anti-HBs adsorbed onto the MI-CMs decreased when the flow-rate through the column increased [25]. The adsorption capacity significantly decreased from 321.0 mIU/g CM to 144.5 mIU/g CM when flow-rate increased from 0.50 mL/min to 2.0 mL/min. Similarly, the adsorption capacity of NI-CMs were decreased from 208.1 mIU/mL to 87.6 mIU/mL in same flow-rate range. The results are due to decrease in contact time between the anti-HBs molecules and the MI-CMs at higher flow rates. The residence time of the anti-HBs in the CM is getting longer when the flow-rate decreased. Thus, the anti-HBs molecules have more time to diffuse to the pore walls of the CMs, to interact with embedded particles and to bind to the molecular cavities at lower flow-rates, hence a better adsorption capacity is observed. It should be noted that there is no pressure drop limitation because of supermacroporous characters of the CMs [33,34].

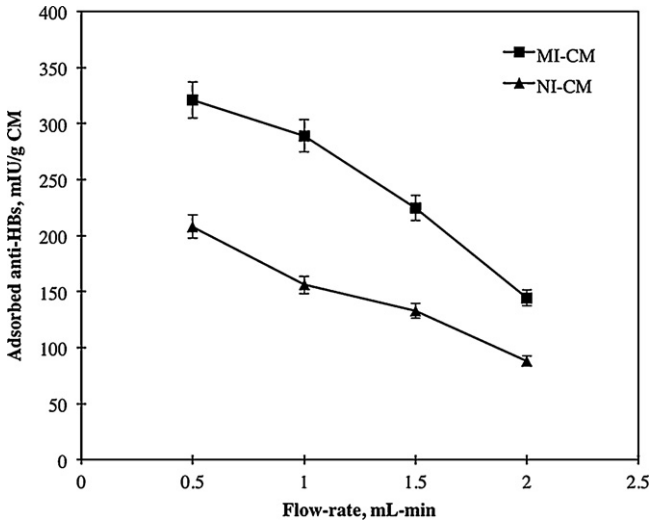

Fig. 3. The adsorption dependency on flow-rate of the MI-CMs and NI-CMs. Anti-HBs concentration: 44.75 mIU/mL; *T*: 25 °C.

3.2.2. Effect of initial anti-HBs concentration

The adsorption dependency of the MI-CMs and NI-CMs are given as a function of anti-HBs concentration (Fig. 4). As seen in this figure, the increase in the anti-HBs concentration in plasma causes an increase in the adsorption capacities of the MI-CMs and the NI-CMs. The maximum adsorption capacities of the MI-CMs and the NI-CMs are achieved as 700.2 mIU/g and 427.8 mIU/g, respectively. This fact depended on the driving force derived from concentration difference between liquid and solid phases. By increase in the concentration, the concentration gradient is getting stronger; hereby, the adsorption tendency of the analyte molecules, anti-HBs, is also inclined [35]. In addition, the results show that anti-HBs molecules easily move through inter-connected channels of CMs, reaching to and interacting with specific cavities of the embedded porous particles and binding to interaction binding sites (i.e. antibody imprinted cavities) [27]. Here, it should be emphasized the adsorption process was occurred quickly. The process almost reached equilibrium in first 30 min (Supplementary Material, SM-Fig. 2). Higher adsorption capacity of CMs was stemmed from several important parameters controlling adsorption process. First, whole solution directly flows through cryogel structure that was retained after

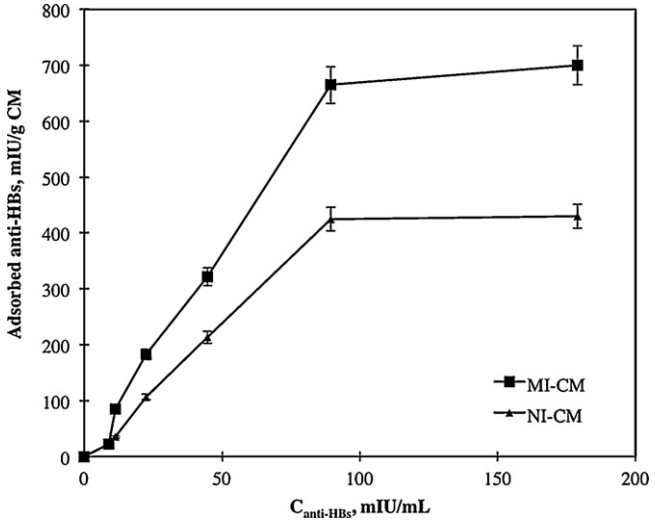

Fig. 4. The adsorption dependency on concentration of the MI-CMs and NI-CMs. Flow-rate: 0.50 mL/min; *T*: 25 °C.

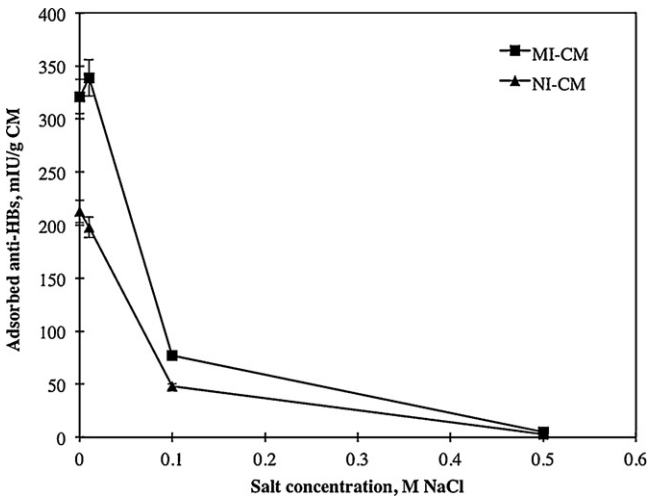

Fig. 5. The effect of salt concentration on anti-HBsAb adsorption capacity of the MI-CMs. Anti-HBs concentration: 44.75 mIU/mL; flow-rate: 0.50 mL/min; *T*: 25 °C.

cryogelation although embedding process. Therefore, anti-HBs molecules effectively diffuse into and interact with imprinted cavities or functional monomer. Second, embedding of particles into cryogel structure increased specific surface area, numbers of imprinted cavities for anti-HBs molecules. Third, convective flow allows anti-HBs molecules to move through interconnected supermacropores of the cryogels easily and adsorb on the imprinted cavities specifically. Fourth, diffusion and mass transport limitations were also reduced because of convective flow. In addition, surface film that is most rate-limiting step of the adsorption processes exterior of the cryogel was thickener which accelerates the adsorption because of convective transport of anti-HBs molecules. The combination of these parameters makes a synergic effect that causes faster adsorption process and higher adsorption capacities.

3.2.3. Effect of ionic strength

The effect of NaCl concentration on the adsorption capacity of the MI-CMs and the NI-CMs was also investigated. High ionic strengths weakened the binding as shown in binding experiments when increasing amounts of NaCl were added to the adsorption solution (Fig. 5). Anti-HBs adsorption capacity of the MI-CMs and the NI-CMs decreased from 338.0 mIU/g to 4.81 mIU/g for MI-CMs and from 213.0 mIU/g to 3.11 mIU/g for NI-CMs when the NaCl concentration increased to 0.5 M. According to the results, ionic interactions gave an essential contribution to the recognition and binding process [36]. A possible explanation for this phenomenon could be in two ways; (i) Counter salt ions interact with the anti-HBs molecules via charge-charge interactions and mask the binding sites, and (ii) decrease in the adsorption capacity due to the increase in ionic strength can be attributed to the repulsive electrostatic forces between the MI-CMs and anti-HBs molecules [37].

3.2.4. Selectivity experiments

In order to show the selectivity of the CMs, a competitive adsorption was performed from anti-HBs and anti-HAV positive plasma. For this purpose, anti-HBs, total anti-HAV antibody (anti-HAV IgG + IgM) and total IgE adsorption capacities of the MI-CMs were evaluated. Anti-HAV antibody was chosen as a competitive protein to show selectivity between two different hepatitis types. IgE molecule, another Y shape immunoglobulin molecule, was chosen to show the selectivity of molecular shape. The selectivity constants (K_d, k and k') were summarized in Table 2.

If K_d values were considered, the distribution constant of anti-HBs molecules is higher than that of other molecules for the MI-CMs

Table 2
K_d, k and k' values of the MI-CMs and the NI-CMs.

	MI-CMs		NI-CMs		k'
	K_d	k	K_d	k	
Anti-HBs	10.25	–	7.31	–	–
Total anti-HAV	5.28	1.94	20.54	0.36	5.45
Total IgE	2.26	4.54	14.59	0.50	9.05

Anti-HBs: 895 mIU/mL; total anti-HAV: 490 mIU/mL; total IgE: 5000 mIU/mL. Dilution factor is one hundred fold.

as opposed to the NI-CMs. k values which show the distribution of anti-HBs molecule due to the interfering molecules were calculated as 1.94 for total anti-HAV antibody and 4.54 for total IgE molecules for the MI-CMs. In the case of NI-CMs, these values were calculated as 0.36 for total anti-HAV antibody and 0.50 for total IgE molecules. These results show that the template molecules, anti-HBs, have been recognized by MI-CMs. The relative selectivity constant (k') that is another parameter for evaluation of performance of the imprinted adsorbents was calculated as 5.45 for anti-HBs due to total anti-HAV and 9.05 for anti-HBs due to total IgE, respectively. These mean that MI-CMs can specifically recognize and adsorb anti-HBs molecules as 5.45-folds according to total anti-HAV and 9.05-folds according to total IgE, respectively. Therefore, it can be concluded that the MI-CMs have higher selectivity to anti-HBs molecules considering not only antibodies against two different hepatitis types, A and B, but also Y-shaped antibodies molecules, IgE and anti-HBs. As a result, we can conclude that the anti-HBs imprinted cavities in the CMs recognize and identify the anti-HBs molecules more specifically.

3.2.5. *Reusability and stability of the cryogel membranes*

In order to show the stability and reusability of the MI-CMs, the adsorption–elution cycle from human plasma was repeated ten times using the same CM 1 h for each elution cycle. The CM was washed with 50 mM NaOH solution for 30 min for sterilization after each adsorption–elution cycle. After that, the CM was washed with distilled water for 30 min, then, equilibrated with the 0.1 M phosphate buffer at pH 7.4 for the next adsorption–elution cycle. As seen in Fig. 6 that the cryogel is very stable and maintain their adsorption capacity almost constant as more than 95.0%. The result indicates that recognition, interaction and adsorption processes are occured reversibly and the methods applied for elution and equilibration are convenient for purification procedure. In addition, this high performance of the MI-CMs regarding to parameters such as scaling-up and lowering the cost of the purification process makes them a promising candidate for large scale anti-HBs purification technology.

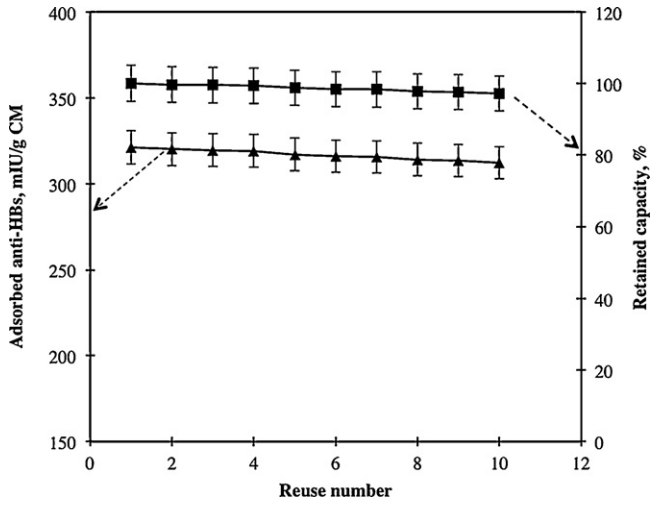

Fig. 6. Reusability and stability of the MI-CMs. Anti-HBs concentration: 44.75 mIU/mL; flow-rate: 0.50 mL/min; desorption buffer: phosphate 7.4 including 1.0 M NaCl; T: 25 °C.

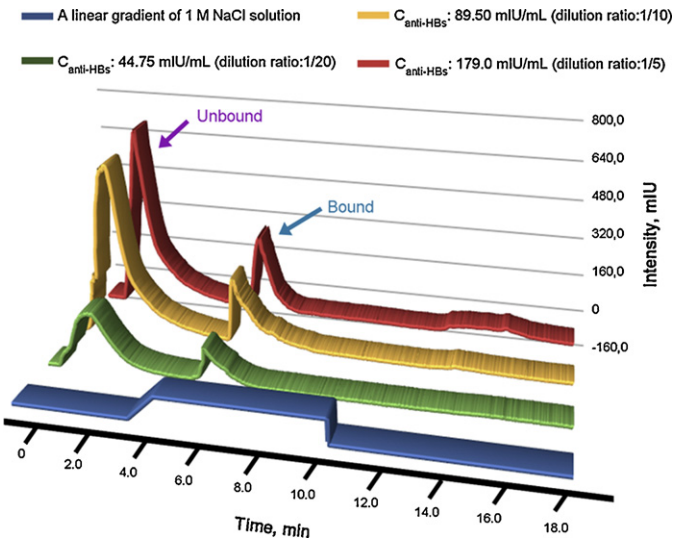

Fig. 7. FPLC purification of anti-HBs from human plasma by the MI-CMs. Flow rate: 1.0 mL/min; anti-HBs concentration: 44.75–179.0 mIU/mL; equilibration buffer: 100 mM phosphate at pH 7.4; eluent solution: a linear gradient of NaCl in 100 mM phosphate buffer (pH 7.4) from 0.0 to 1.0 M; detection was performed at 280 nm.

Table 3
Anti-HBs activities (mIU/mL) of the FPLC fractions.

Dilution factor,[a] fold	Anti-HBs activity (mIU/mL)		Retention efficiency (%)
	Bound	Unbound	
20	31.73	12.89	71.11
10	59.45	31.12	65.64
5	99.28	78.45	55.86

[a] Undiluted plasma concentration of Anti-HBs: 895 mIU/mL.

3.3. *FPLC studies*

In order to evaluate the chromatographic purification performance of the MI-CMs, we have connected them to FPLC system. As seen in Fig. 7, we have applied anti-HBs positive plasma samples diluted in different ratios to FPLC system. Frac920 fraction collector unit used for collecting the peaks, bound and unbound regions of the chromatogram. The anti-HBs activities of each fraction were determined as mentioned before (Table 3). As seen in Table 3, the MI-CMs have the retention capacities in range of 55.86–71.11% with respect to initial anti-HBs concentration. Table 4 shows the parameters calculated from the purification chromatograms. As summarized in table, anti-HBs molecules were eluted from the MI-CMs at 6.35 min while unbound fraction came out at 1.87 min. The theoretical plate number (N) and capacity factor (CF) of the MI-CMs were calculated as 1153.9 and 5.48 for anti-HBs molecules, respectively. The other parameters indicating resolution and separation performance were determined as 1.72 and 6.02, respectively. These results consolidate and confirm that the separation of the anti-HBs

Table 4
The parameters calculated from the purification chromatograms.

	t_R	N	CF	α	R_s
Anti-HBs (bound fraction)	6.35	1153.90	5.48	–	–
Competitors (unbound fraction)	1.87	4.11	0.91	6.02	1.72

molecules from plasma was achieved successfully by using MI-CMs as continuous separation media.

4. Conclusion

It is hard to imprint the proteins into polymeric matrix because of their tendencies to denaturation and conformational change during the polymerization. One of the proposed methods to solve these problems is to carry out the polymerization under mild condition such as low temperature [4]. Cryogels are the prominent alternatives; because, not only offering solution to the mentioned problems but also serving unique properties such as large inter-connected flow channels, low back pressure, low diffusion resistance, rapid and efficient adsorption dynamics for separation and purification of interested molecules [38–40]. In this study, we aimed to prepare molecular imprinted cryogel membranes for chromatographic purification of anti-HBs molecules from human plasma. These molecules were used to immunize passively the infants born to hepatitis B carrier mother and people who need an immediate protection [7,41]. As large scale antibody purification protocols, the anti-HBs molecules were also purified via this method [4,42]. According to our results, the offered cryogel membranes can be classified as potential alternative for conventional competitors because of their encouraging properties such as high adsorption capacity, specific ability to recognize anti-HBs molecules, rapid adsorption kinetics, chemical and physical stability and reusability while retaining capacity more than 95% after 10 adsorption–desorption cycle, low flow and diffusion resistance etc. Finally, it can be concluded that MI-CMs could be used for specific purification of anti-HBs from anti-HBs positive human plasma and classified as a promising alternative for large-scale purification.

Appendix A. Supplementary data

Supplementary data associated with this article can be found, in the online version, at doi:10.1016/j.jchromb.2012.02.001.

References

[1] R.A. Heijtink, P. van Bergen, M.H. van Roosmalen, C.M.G. Sunnen, W.P. Paulij, S.W. Schalm, A.D.M.E. Osterhaus, Vaccine 19 (2001) 3671.
[2] W.F. Carman, J. Viral Hepat. 4 (1997) 11.
[3] H.Y. Hsu, M.H. Chang, S.H. Liaw, Y.H. Ni, H.L. Chen, Hepatology 30 (1990) 1312.
[4] L. Uzun, R. Say, S. Unal, A. Denizli, J. Chromatogr. B 877 (2009) 181.
[5] F. Maeda, M. Takekoshi, Y. Nagatsuka, S. Aotsuka, M. Tsukahara, A. Ohshima, I. Kido, Y. Ono, S. Ihara, J. Virol. Methods 127 (2005) 141.
[6] K. Shiraki, J. Gastroenterol. Hepatol. 15 (2000) 11.
[7] R. Zachoval, W. Jilg, B. Lorbeer, M. Schmidt, F. Deinhrdt, J. Infect. Dis. 150 (1984) 112.
[8] A.J. Zuckerman, Br. Med. Bull. 46 (1990) 383.
[9] R. Hernandez, L. Plana, L. Gomez, N. Exposito, J. Valdes, R. Paez, E. Martinez, A. Beldrarain, J. Chromatogr. B 816 (2005) 1.
[10] S.D.S. Mouta Junior, C.O.A. Vianna, I. Ennes, S.D.A. Gomes, M.D.S. Freire, E.D.D. Silva, S.G.D. Simone, M.T.B.D. Moraes, J. Chromatogr. B 787 (2003) 303.
[11] M. Pujol, N.I. Ramirez, M. Ayala, J.V. Gavilondo, R. Valdes, M. Rodriguez, J. Brito, S. Padilla, L. Gomez, B. Reyes, R. Peral, M. Perez, J.L. Marcelo, L. Mila, R.F. Sanchez, R. Paez, J.A. Cremata, G. Enriquez, O. Mendoza, M. Ortega, C. Borroto, Vaccine 23 (2005) 1833.
[12] A. Leyva, A. Franco, T. Gonzales, J.C. Sanchez, I. Lopez, D. Gaeda, N. Hernandez, M. Montanes, I. Delgado, R. Valdes, Biologicals 35 (2007) 19.
[13] A. Yano, F. Maeda, M. Takehoshi, J. Med. Virol. 72 (2004) 208.
[14] H. Yavuz, A. Denizli, Macromol. Biosci. 5 (2005) 39.
[15] L. Uzun, D. Turkmen, V. Karakoc, H. Yavuz, A. Denizli, J. Biomater. Sci. 22 (2011) 2325.
[16] L. Uzun, R. Say, S. Unal, A. Denizli, Biosens. Bioelectron. 24 (2009) 2878.
[17] M.J. Whitcombe, I. Chianella, L. Larcombe, S.A. Piletsky, J. Noble, R. Porter, A. Horgan, Chem. Soc. Rev. 40 (2011) 1547.
[18] L. Chen, S. Xu, J. Li, Chem. Soc. Rev. 40 (2011) 2922.
[19] N.W. Turner, C.W. Jeans, K.R. Brain, C.J. Allender, H. Hlady, D.W. Britt, Biotechnol. Prog. 22 (2006) 1474.
[20] A. Poma, A.P.F. Turner, S.A. Piletsky, Trends Biotechnol. 28 (2010) 629.
[21] G. Sener, E. Ozgur, E. Yilmaz, L. Uzun, R. Say, A. Denizli, Biosens. Bioelectron. 26 (2010) 815.
[22] Y. Ge, A.P.F. Turner, Trends Biotechnol. 26 (2008) 218–224.
[23] G. Erturk, L. Uzun, M.A. Tumer, R. Say, A. Denizli, Biosens. Bioelectron. 28 (2011) 97.
[24] N. Bereli, M. Andaç, G. Baydemir, R. Say, I.Y. Galaev, A. Denizli, J. Chromatogr. A 1190 (2008) 18.
[25] S. Asliyuce, N. Bereli, L. Uzun, M.A. Onur, R. Say, A. Denizli, Sep. Purif. Technol. 73 (2010) 243.
[26] N. Bereli, G. Şener, E.B. Altıntaş, H. Yavuz, A. Denizli, Mater. Sci. Eng. C 30 (2010) 323.
[27] K. Tekin, L. Uzun, Ç.A. Şahin, S. Bektaş, A. Denizli, React. Funct. Polym. 71 (2011) 985.
[28] H. Kirsebom, B. Mattiasson, I.Y. Galaev, Langmuir 25 (2009) 8462.
[29] H. Kirsebom, D. Topgaard, I.Y. Galaev, B. Mattiasson, Langmuir 26 (2010) 16129.
[30] Y. Wang, B. Liu, Biosens. Bioelectron. 24 (2009) 3293.
[31] N. Basar, L. Uzun, A. Guner, A. Denizli, Int. J. Biol. Macromol. 41 (2007) 234.
[32] L.I. Grace, R. Cohen, T.M. Dunn, D.M. Lubman, M.S. De Vries, J. Mol. Spectrosc. 215 (2002) 204.
[33] L. Uzun, A. Denizli, J. Biomater. Sci. 17 (2006) 791.
[34] H. Alkan, N. Bereli, Z. Baysal, A. Denizli, Biochem. Eng. J. 45 (2009) 201.
[35] M.M. Sarı, C. Armutcu, N. Bereli, L. Uzun, A. Denizli, Colloids Surf. B 84 (2011) 140.
[36] H. Alkan, N. Bereli, Z. Baysal, A. Denizli, Biochem. Eng. J. 51 (2010) 153.
[37] E.B. Altıntaş, A. Denizli, Int. J. Biol. Macromol. 38 (2006) 99.
[38] I. Percin, E. Saglar, H. Yavuz, E. Aksoz, A. Denizli, Int. J. Biol. Macromol. 48 (2011) 577.
[39] E. Bayram, L. Uzun, D. Turkmen, E. Yılmaz, I.Y. Galaev, A. Denizli, S. Bektas, Hacettepe J. Biol. Chem. 35 (2007) 219.
[40] A. Denizli, Hacettepe J. Biol. Chem. 39 (2011) 93.
[41] A. Denizli, Hacettepe J. Biol. Chem. 39 (2011) 213.
[42] A. Denizli, Hacettepe J. Biol. Chem. 39 (2011) 1.